

1 IVIVE-PBPK based New Approach Methodology for addressing early life  
2 toxicity induced by Bisphenol A

3  
4 Mengmei Ni<sup>a,b</sup>, Deepika Deepika<sup>b,c</sup>, Xiaomeng Li<sup>a</sup>, Wei Xiong<sup>a</sup>, Lishi Zhang<sup>a</sup>, Jinyao Chen<sup>a,\*</sup>,  
5 and Vikas Kumar<sup>b,c,d\*</sup>

6  
7 <sup>a</sup>*West China School of Public Health/West China Fourth Hospital and Healthy Food*  
8 *Evaluation Research Center, Sichuan University, Chengdu, China*

9 <sup>b</sup>*Environmental Engineering Laboratory, Departament d' Enginyeria Quimica,*  
10 *Universitat Rovira i Virgili, Av. Paisos Catalans 26, 43007, Tarragona, Catalonia,*  
11 *Spain*

12 <sup>c</sup>*IISPV, Hospital Universitari Sant Joan de Reus, Universitat Rovira i Virgili, Reus,*  
13 *Spain*

14 <sup>d</sup>*German Federal Institute for Risk Assessment (BfR), Max-Dohrn-Str. 8-10, 10589*  
15 *Berlin, Germany*

16 **Abstract**

17 Bisphenol A (BPA) is a known endocrine disruptor mimicking natural estrogens with the potential  
18 to affect human health, especially during prenatal and postnatal exposure at or below current  
19 acceptable daily intake levels. Different adverse effects of BPA are still under investigation, and  
20 multiple mechanisms of action remain unexplored. This may be one of the reasons for the  
21 continuously changing tolerable daily intake (TDI) of BPA with the emergence of new adverse  
22 health effects over time. In addition, translational modelling through in vitro-in vivo extrapolation  
23 (IVIVE) can act as prerequisite bridge for translating in-vitro finding into human risk assessment.  
24 The objective of this study was to conduct in-vitro experiments and utilize an IVIVE-pregnancy  
25 physiologically based pharmacokinetic (P-PBPK) modeling to investigate developmental  
26 neurotoxicity and embryotoxicity in humans. The data obtained from human embryonic stem cells-  
27 based assays (study conducted between October 2020-2021) were used for the IVIVE-P-PBPK  
28 models to obtain the human equivalent doses (HEDs) which were further extrapolated to reference  
29 doses (RfDs). The results showed that simulated mean RfDs ( $\mu\text{g}/\text{kg}/\text{day}$ ) derived from the HSD3B1  
30 and NFATC2 gene of embryotoxicity and neurodevelopmental toxicity tests, respectively, were 4.94  
31 and 5.18. The simulated RfDs were close to the temporary-tolerable daily intake (t-TDI)  
32 recommended by European Food Safety Authority (EFSA) in 2015 (t-TDI:  $4 \mu\text{g}/\text{kg}\cdot\text{bw}$ ) and higher  
33 than the TDI of 2023 ( $0.2 \text{ ng}/\text{kg}\cdot\text{bw}$ ). In conclusion, in-vitro toxicogenomics dose-response data  
34 combined with PBPK modeling can become a promising alternative new approach methodology  
35 (NAM) to support decision-making in chemical risk assessment. Based on the simulated RfDs  
36 derived from this NAM, the t-TDI set by EFSA in 2015 may be considered a safe exposure limit for  
37 mothers and fetuses at the current BPA intake levels in Chinese mothers. This study provided an  
38 animal-free new strategy for NAMs based risk assessment by combining toxicogenomics and  
39 computational toxicology.

40  
41 **Key words:** Bisphenol A; IVIVE, PBPK; Embryotoxicity; Neurotoxicity; human embryonic stem

42 cells; toxicogenomics

43

## 44 1. Introduction

45 Bisphenol A (BPA) is a synthetic endocrine disruptor widely used to manufacture  
46 polycarbonate plastics and epoxy resins since the early 1950s<sup>1</sup>. It is often used in plastic containers,  
47 toys, baby bottles, electrical equipment, medical devices, and much more<sup>2, 3</sup>. With the continuously  
48 growing demand for BPA production, the global BPA market is estimated to have a value of 30.62  
49 billion dollars by 2026<sup>4</sup>. BPA is highly prevalent in the environment and has been found in water  
50 (surface water, river water, groundwater, wastewater, and freshwater), sediments and soil samples  
51 worldwide<sup>5</sup>. A recent study in Mexico showed a BPA concentration of 148–9340 ng/L in water  
52 samples used for the irrigation of crops<sup>6</sup>. China has the highest concentration of BPA in lake  
53 sediments, ranging from 1.1 to 270 ng/g dry weight<sup>7</sup> and in soil ranging from 72,500 to 198,000  
54 ng/g·dw<sup>8</sup>. Humans can be exposed to BPA via ingestion through food (vegetables, fruits, fish, meat,  
55 canned food and infant food) which remains the major source of exposure followed by dermal and  
56 inhalation<sup>9, 10</sup>.

57 As an endocrine-disrupting chemical (EDC), BPA can disrupt the hormonal system and also  
58 exerts a harmful impact on human health by affecting reproductive, developmental, immunological,  
59 and neurological functions<sup>11-14</sup>. BPA is being detected in human urine, blood, amniotic fluid, breast  
60 milk and other biological specimens<sup>14-16</sup>. The fetal development stage is known to be the critical  
61 period of vulnerability to BPA exposure<sup>17</sup>, which may result in adverse birth outcomes<sup>18</sup>.

62 Many countries worldwide have issued strict regulations to limit BPA exposure<sup>19, 20</sup>.  
63 Regulatory authorities from Canada and Europe have banned the BPA use in polycarbonate infant  
64 feeding bottles<sup>21</sup>. A specific migration limit (SML) of 0.05 mg of BPA per kg of food was established  
65 by the E.U. in February 2018 to avoid migration from varnishes or coatings applied to food  
66 packaging materials (No 2018/213). The U.S. Food and Drug Administration (FDA) announced that  
67 BPA could no longer be used in baby bottles and sippy cups in 2012. Also, the European Food Safety  
68 Authority (EFSA) has continuously decreased the tolerable daily intake (TDI) of BPA over the years.  
69 In 2006, the temporary-tolerable daily intake (t-TDI) of 50 µg/kg bw/day was set based on the  
70 reduced body weight in rats<sup>22</sup> which was reduced to 4 µg/kg bw/day in 2015 based on the increase  
71 in relative kidney weight<sup>23</sup>. In the recent scientific opinion of 2023, EFSA established the TDI to  
72 0.2 ng/kg bw based on immune toxicity in mice<sup>24, 25</sup>. The continuous reduction in TDI over the years  
73 emphasizes the need to fully elucidate the adverse effects of BPA on human health especially in  
74 sensitive age-groups. The traditional risk assessment is mainly based on animal testing, which is  
75 time-consuming and expensive and is not in accordance with the Three Rs principles (replacement,  
76 reduction and refinement)<sup>26</sup>. The other concerns are the uncertainty in dosimetry, extrapolation from  
77 animal to human due to different toxicokinetics, and extrapolating high-dose effects in animals to  
78 low-dose human exposures<sup>27</sup>. Moreover, the adverse effects found in animal testing may not  
79 represent the most sensitive toxic effects for the human population especially the fetus, leading to  
80 an underestimation of safety limits. To reduce these uncertainties, in-vitro cell line data translated  
81 with in-vitro to in-vivo extrapolation (IVIVE)- physiologically based pharmacokinetic model  
82 (PBPK) for humans can be a good alternative. For studying developmental toxicity, embryonic stem  
83 cells (ESCs) are considered good models as they can proliferate fast and have the ability to  
84 differentiate into any types of somatic cells<sup>28, 29</sup>. In addition, human ESCs avoid bias in interspecies  
85 differences and may have better predictability for human risk assessment compared to animal ESCs.

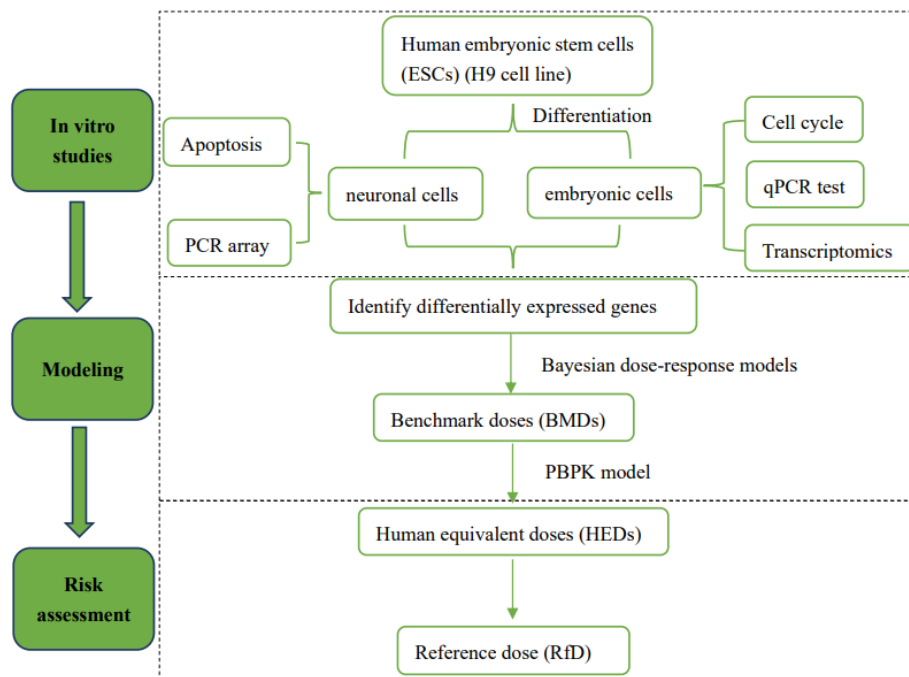
86 The new approach methodology (NAM) has started gaining popularity to enable translation for

87 regulatory decision-making after the publication of NRC report on “Toxicity Testing in the 21st  
88 Century”<sup>30, 31</sup>. Currently, the IVIVE is being used to quantitatively extrapolate in-vitro experimental  
89 results to predict in-vivo biological effects and translate to human equivalent doses (HEDs)<sup>32-34</sup>.  
90 IVIVE-PBPK is one of the applications for translation of in-vitro data which falls under NAMs  
91 since it can reduce experimental studies, especially testing in animals. There have been few studies  
92 in the past utilizing this approach for assessing risk. For instance, Chen et al.<sup>35</sup> used differentially  
93 expressed gene (DEG) data from literature of mouse in-vivo and human in-vitro toxicogenomic to  
94 convert to reference doses (RfDs) using PBPK model for PFOS chemical. Zhang et al.<sup>36</sup> integrated  
95 cell-based assays with a PBPK model combined with the Monte Carlo method to conduct health  
96 risk assessment of cadmium exposure. Lin et al.<sup>37</sup> converted ToxCast in vitro estrogen receptor (ER)  
97 assays to HEDs of multiple BPs (BPA, BPS, BPF, and BPAF) by a population-based IVIVE  
98 extrapolation using PBPK models coupled with Monte Carlo simulations. The objective of this study  
99 was to utilize Human ESCs to conduct experiments after BPA exposure for evaluating toxicity in  
100 embryos and developing brains. The toxicogenomic data produced in the study was used to obtain  
101 dose response through benchmark dose analysis. A Pregnancy PBPK (P-PBPK) model was used to  
102 calculate the HED and later RfD to compare with the established regulatory guidelines. This is one  
103 of the studies of its kind where human cell-based toxicogenomic data for developmental  
104 neurotoxicity (DNT) and embryo toxicity was utilized for risk assessment. Such studies in future  
105 may reduce the dependence on animal testing by integrating in-vitro with computational models and  
106 reduce inter- and intraspecies variability.

## 107 108 2. Methods

109 A conceptual diagram of this study is shown in Figure 1. The schematics followed for this study are  
110 as follows:

- 111 1) In vitro studies: Human ESCs (H9 line) were differentiated into two types of cells——  
112 neuronal cells and embryonic cells. The equivalent cell dose was calculated using the P-  
113 PBPK model, considering exposure in adult women in the Chinese population. Both types  
114 of cells were exposed to different concentrations of BPA for 14 days during differentiation.  
115 Cell cycle, qPCR tests and transcriptomics were performed for embryonic cells, while  
116 apoptosis and PCR array analysis was conducted for neuronal cells. Toxicogenomic dose-  
117 response data was collected and used further for modeling.
- 118 2) BMD and P-PBPK Modeling: DEGs were identified by integrating and calculating the  
119 above experimental results. The BMD approach was used to conduct the dose-response  
120 modeling with PCR data of DEGs. The gene BMD<sub>5</sub> was calculated as POD to derive HED.  
121 The POD was used as input for the P-PBPK model to reconstruct exposure for deriving  
122 HEDs (The detailed calculation is shown in 2.3).
- 123 3) Risk assessment: The RfDs were calculated using simulated HEDs and by considering an  
124 additional uncertainty factor of 10 (The detailed calculation is shown in 2.4). The  
125 calculated RfDs were compared with the TDI of BPA set by EFSA to evaluate the risk for  
126 the fetus.



127  
128  
129  
130  
131  
132  
133  
134

Figure 1. Framework of the study integrating in-vitro data with in-silico model for risk assessment. First, BPA-induced neuronal and embryonic dose-response data were obtained from in vitro studies. Second, the differentially expressed genes were identified and analysed using the Bayesian benchmark dose (BMD) method. The internal dosimetry and the human equivalent doses (HEDs) were subsequently calculated using a published PBPK model. Third, the reference doses (RfDs) for HEDs of different genes associated with BPA exposure were calculated.

## 135 In-vitro experiments

### 136 2.1.1 Cell culture and treatment

#### 137 Treatment of H9 cells

138 Human ESCs (H9 cell line) were obtained from Applied Cell (Shanghai, China). The cells were  
139 cultured with matrigel human ESC-qualified Matrix (Corning, Arizona, US) under feeder-  
140 independent conditions and grown in mTeSR™ Plus (Stemcell Technologies, Vancouver, Canada)  
141 at 37°C and 5% CO<sub>2</sub>. The manufacturer's protocol was followed for maintaining, expanding  
142 culturing, and passaging the cells. Further details have been provided in (Supplementary file 1).

#### 143 Differentiation of embryonic cells

144 The formation and differentiation of embryoid bodies (EBs) were derived from H9 cells, which  
145 was based on a previous description<sup>42</sup>. Briefly, single H9 cells were obtained from H9 clones and  
146 cultured with the EB formation medium (StemCell Technologies, Inc.) in an AggreWell™ plate for  
147 2 days. EBs were then collected and placed in an ultra-low adherence 6-well plate with the EB  
148 suspension culture medium (knock-out DMEM, supplemented with 20% knockout serum, 1%  
149 nonessential amino acids, 2 mM L-glutamine and 0.1mmol/L mercaptoethanol) for 3 days. On day  
150 5, EBs were plated in the EB adherent medium (90% DMEM, 10% fetal calf serum and 4mM L-  
151 glutamine) for 11 days. EBs were exposed to BPA for two weeks, starting from the day of EB  
152 formation.

#### 153 Differentiation of neuronal cells

154 For the generation of neuronal cells, the differentiation process was performed according to

155 the manufacturer's protocol. A single-cell suspension of H9 cells was collected in AggreWell™800  
156 24-well Plate to generate EBs with STEMdiff™ SMADi Neural Induction. Daily partial (1/2)-  
157 medium was changed. After 5 days, EBs were harvested and plated onto matrix-coated wells of a  
158 tissue culture-treated 6-well plate. After 7 days, neural rosette selection and replating were  
159 conducted to form neuronal precursors. A daily full-medium change with warm (37°C) STEMdiff™  
160 Neural Induction Medium + SMADi was performed for 7 days. Then the neuronal precursors were  
161 passaged using STEMdiff™ forebrain neuron maturation medium for neuron maturation. Neurons  
162 were exposed to BPA with STEMdiff™ forebrain neuron maturation medium for two weeks, starting  
163 from the day of neuron maturation.

164

### 165 2.1.2 Cell viability assay and PBPK modeling for dose setting

166 For cell viability assay, H9 single cells were plated into a 96-well plate with 3000 cells/well.  
167 After 24 hours, cells were exposed to 0, 50, 75, 100, 125, 150, 200, and 250 µM BPA for 7 days, 6  
168 wells for each exposed group. The medium was replaced every other day. On the 7<sup>th</sup> day, cell  
169 viability was measured using the Cell-Counting-Kit 8 test kit (Dojindo, Japan).

170 The minimum test dose for embryonic (0.05 nM) and nerve cells (0.014 nM) was calculated  
171 from a previously developed and validated P-PBPK model. This was done by converting a female  
172 oral dose of 218.320 ng/kg bw/day (the oral dose represents the average dietary exposure level of  
173 BPA in adult women between 20-50 years old reported in the fifth total dietary study of China<sup>40</sup>)  
174 into internal exposure doses during pregnancy. Since the test cells are embryonic and neuronal cells,  
175 amniotic fluid and fetus's brain were selected as the target sites for calculating internal exposure  
176 doses using total Area under Curve (AUC<sub>total</sub>) (Supplementary file 2, Figure S1). The pregnancy  
177 scenarios were set as gestation day (GD) 56 for embryonic cells (the first trimester was chosen as  
178 ESCs only exist in the early stages of embryonic development), and GD 245 (the third trimester was  
179 chosen as the fetus's brain has not developed until the third trimester) for neuronal cells. Further  
180 details about the model have been provided in the supplementary file along with major equations  
181 (Supplementary file 3). Additional details can be found in the original publication<sup>38</sup>. Other exposure  
182 routes were not considered as dietary exposure is the major contributor to BPA exposure in humans.  
183 Since the BPA dietary exposure of pregnant women was not available in the fifth Chinese Total diet  
184 study (TDS), the dietary exposure of BPA in adult women between 20-50 years old was used. In  
185 this model, the height and weight of Chinese adult women were set at 158 cm and 59 kg,  
186 respectively<sup>41</sup>. The t-TDI of BPA established by EFSA in 2015 is 4 µg/kg·bw and was also used to  
187 obtain the equivalent test dose (1 nM for embryonic cells, 0.256 nM for nerve cells) using the P-  
188 PBPK model. These doses were set as the initial concentrations for the embryonic and  
189 neurodevelopmental toxicity test. Considering the cell viability assay results and given that  
190 embryonic cell is naturally differentiated from H9 cells, the maximum dose of the embryonic cell  
191 was set to 30 µM. Similarly, the maximum dose for nerve cells was set at 100 µM. Finally,  
192 embryonic cells were treated with 0, 0.05 nM, 1 nM, 100 nM, 10 µM, and 30 µM BPA; for nerve  
193 cells, the doses were set as 0, 0.014 nM, 0.256 nM, 50 µM, 75 µM, and 100 µM BPA.

194

### 195 2.1.3 Cell cycle and apoptosis assay

196 The cell cycle assay of embryonic cells was performed using a Cell Cycle Kit (KeyGEN, China,  
197 KGA512). After 14 days of BPA exposure, the embryonic cells were harvested and treated according  
198 to the manufacturer's protocols. The cells were analyzed using Guava InCyte software (version 2.7,  
199 Millipore, USA). Apoptosis of neuronal cells was conducted using Annexin V-FITC/PI Apoptosis  
200 Detection Kit (KeyGEN, China, KGA108-1). After 14 days of exposure to BPA, the neuronal cells

201 were collected and stained according to the manufacturer's procedure. The apoptotic rate was  
202 detected by flow cytometry using Guava InCyte (Millipore, USA).

203

#### 204 2.1.4 Transcriptomics analysis

205 After 14-day of exposure, total RNA of the embryonic cells was collected using TRIzol reagent.  
206 The quantification, purity and integrity of the RNA were assessed using the Agilent Bioanalyzer  
207 system. Then following the manufacturer's instructions of TruSeq Stranded mRNA LT Sample Prep  
208 Kit (Illumina, San Diego, CA, USA), the libraries were constructed. Sequencing and transcriptome  
209 analysis were performed by OE Biotech Co., Ltd. (Shanghai, China).

210 The DESeq (1.20.0) software was used for differential expression analysis. Significant  
211 differential expression was defined as a  $P$  value  $< 0.05$  and fold change  $> 2$  or  $< 0.5$ . In order to  
212 demonstrate the expression patterns of genes across groups and samples, hierarchical cluster  
213 analysis was performed with DEGs. To understand how DEGs interact and relate, their interactions  
214 were incorporated into pathways. On the basis of hypergeometric distribution, Gene Ontology (GO)  
215 enrichment analysis and Kyoto Encyclopedia of Genes and Genomes (KEGG)<sup>43</sup> pathway  
216 enrichment analysis on DEGs were conducted to identify enriched genes and pathways.

217

#### 218 2.1.5 Quantitative real-time PCR test

219 After 14-day exposure to BPA and dimethyl sulfoxide (DMSO), total RNA was extracted from  
220 embryonic and neuronal cells, and cDNA was produced using iScript™ cDNA Synthesis Kit (Bio-  
221 Rad, USA) and a cDNA reverse transcription instrument (Bio-Rad, USA) according to the  
222 manufacturer's instructions. For nerve cells, the human neurodevelopmental-related gene  
223 microarray (Wegene Biotech, Shanghai, China) was used to detect selected 45 genes encoding the  
224 neurodevelopmental system (The genes are listed in Supplementary file 2, Table S1). The Sangon  
225 Biotech primer bank (Shanghai, China) and NCBI primer-BLAST tool  
226 (<https://www.ncbi.nlm.nih.gov/tools/primer-blast/index.cgi>) were used to generate the gene primer  
227 sequences (Supplementary file 2, Table S2) of interest genes. qPCR tests were conducted with  
228 SsoFast Eva Green Kit (Bio-Rad, USA) and the CFX96 Touch real-time system (Bio-Rad, USA).  
229  $2^{-\Delta\Delta Ct}$  method was used to analyse relative target mRNA expressions with GAPDH as an internal  
230 standard.

231

#### 232 2.2 Bayesian dose-response modeling

233 Bayesian benchmark dose (BBMD) analysis<sup>44</sup> (<https://benchmarkdose.com>) was done to  
234 conduct the dose-response modeling with PCR data. All types of fitted models were considered,  
235 including Exponential 2, Exponential 3, Exponential 4, Exponential 5, Hill, Power, Michaelis-  
236 Menten and Linear models. The prior distributions for model parameters were assumed as uniform  
237 distributions. Markov chain Mon Carlo (MCMC) sampling was conducted using the default settings  
238 in BBMD System, with 1 chain for 30,000 iterations. The warmup percentage was set at 50%. A  
239 model-averaged BMD was calculated using continuous data to estimate gene BMDs. A benchmark  
240 response (BMR) of 5% (i.e., the dose corresponding to 5% relative change to the control group) was  
241 defined in our study. The BBMD system can calculate BMD using a model-averaged method, taking  
242 all available models without selection bias. This model-averaged method is also recommended by  
243 the EFSA<sup>45</sup>. Chou et al<sup>46</sup> demonstrated the validity of this BBMD method by comparing it with  
244 traditional U.S. EPA BMD software. The input data of BBMD website is available in Supplementary  
245 file 4.

246

## 247 2.3 Extrapolation of human equivalent dose

248 The gene BMD<sub>5</sub> values of selected biomarkers were used as the POD to derive the HED. As  
249 embryonic and neuronal cells were used to examine the changes in gene expression due to BPA,  
250 plasma and brain concentrations were utilized to estimate HEDs. A previously developed and  
251 validated P-PBPK model for BPA<sup>38</sup> was applied in this study to calculate the concentration-time  
252 profiles for brain and plasma-based IVIVE. The dose metrics of the maximum steady-state plasma  
253 and brain concentration (C<sub>max,ss</sub>) were extracted and then applied for reconstructing the exposure  
254 utilizing the POD as input with equation 1<sup>34, 46, 47</sup>.

$$255 \quad HED (mg/kg/day) = \frac{POD (\mu M) \times 1(mg/kg/day)}{C_{max,ss} (\mu M)} \quad eq. 1$$

256 For reconstructing exposure or reverse dosimetry, MCMC simulation was performed with  
257 100,000 iterations. Four Markov chains were run with the initial 40000 iterations as a burn-in  
258 required for the model to converge from the initial parameter vector and hence, not considered for  
259 the convergence, the remaining (60000) were used as output iterations. The convergence of posterior  
260 parameters was diagnosed by the potential scale reduction factor ( $\hat{R}$ ). A  $\hat{R}$  value of 1.2 or less was  
261 considered as the criterion for the possible convergence<sup>48</sup>.

262

## 263 2.4 Reference Dose Estimation

264 The fifth percentile of estimated HEDs was taken as the threshold dose (TD) for each gene.  
265 Then the TD was divided by an overall uncertainty factor (10 for interindividual variability) to get  
266 the RfD (eq. 2). An uncertainty factor of 10 for intraspecies variability was considered according to  
267 the literature to calculate the RfD<sup>35</sup>.

$$268 \quad RfD (mg/Kg/day) = \frac{TD(mg/kg/day)}{10} \quad eq. 2$$

269

## 270 2.5 Statistical analysis

271 Experimental data from cell viability assay, cell cycle, apoptosis, and PCR were analyzed by  
272 SPSS software (version 20.0, IBM, USA). The results were shown as mean  $\pm$  standard deviation  
273 and were analyzed by one-way ANOVA. After testing the homogeneity of variance, the LSD test  
274 was used to compare the statistical differences between groups. A *P* value less than 0.05 was  
275 considered statistically significant. The figures were generated using Rstudio 2022.12.0 and  
276 GraphPad Prism 5 (GraphPad Software Inc., USA). Simulations related to PBPK model was done  
277 using MCSim under Rstudio (2023.03.0).

## 278 3. Results

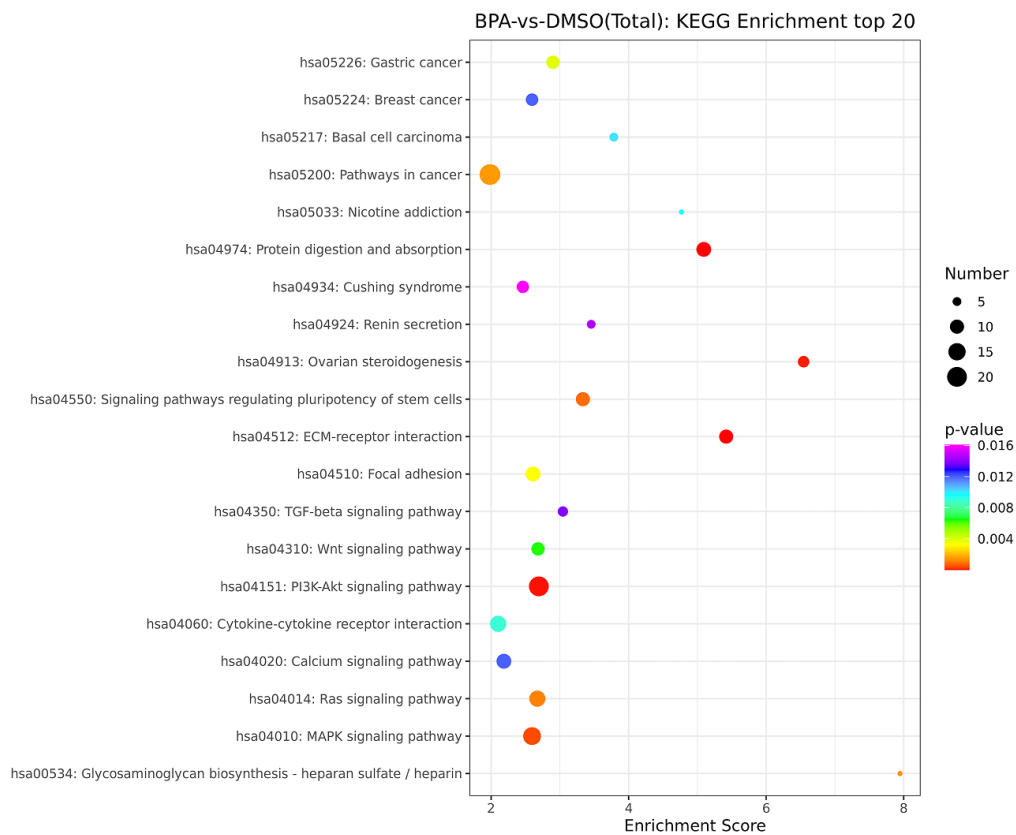
### 279 3.1 Toxicity of BPA on H9-based embryonic/nerve cells

280 The cytotoxicity test was conducted by exposing H9 cells to BPA at 250, 200, 150, 125, 100,  
281 75, and 50  $\mu$ M along with the control. After 1 week of treatment, cells treated with 50- 250  $\mu$ M BPA  
282 showed a significant reduction in viability at 150, 200 and 250  $\mu$ M compared to the control  
283 (Supplementary file 2, Figure S2).

284 The cell cycle of embryonic cells was analyzed after 14 days of treatment. Compared to the  
285 control group, the proportion of G0/G1 cells statistically increased in the 0.05 nM and 30  $\mu$ M groups.  
286 There was no significant difference in S-phase cells between the groups. G2 cells in the 1 nM, 100  
287 nM and 10  $\mu$ M groups were more than that in the control group (Supplementary file 2, Figure S3).  
288 There was no significant difference in the apoptosis test of nerve cells (Supplementary file 2, Table

289 S3).

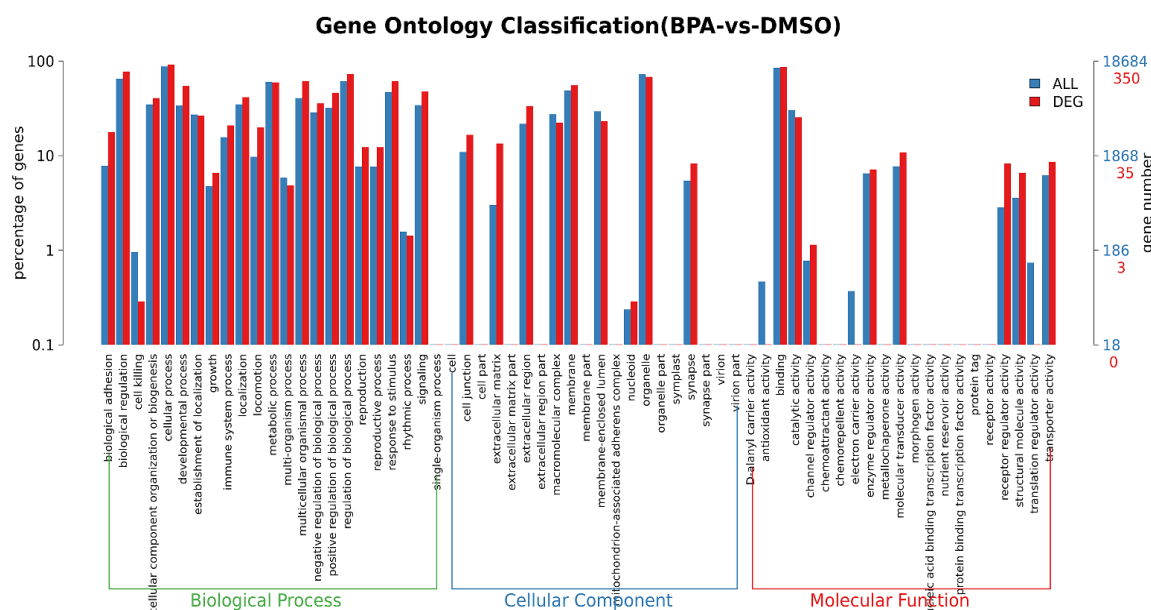
290 From the transcriptomics of the embryotoxicity test, the DEGs number between DMSO control  
291 group and 10  $\mu$ M BPA was 359 ( $q$ -value $<0.05$  &  $|\log_2FC|>1$ ) after 14-day exposures. Of these, 301  
292 genes were up-regulated, and 58 genes were down-regulated among the total genes. KEGG  
293 enrichment analysis showed that the DEGs were involved in many pathways (Figure 2), including  
294 ovarian steroidogenesis, ECM-receptor interaction, phosphatidylinositol 3-kinase (PI3K)-AKT  
295 signaling pathway, etc. GO classification analysis (Figure 3) showed that most DEGs were present  
296 in biological processes, rather than cellular components or molecular functions.



297

298 Figure 2. KEGG enrichment top 20 from embryo toxicity test. The horizontal axis in the  
299 figure represents the enrichment score. The vertical axis represents the top 20 toxicity pathways  
300 (with pathway number and name) in KEGG. The larger the bubble, the more differential protein  
301 coding genes the pathway contains. The color of the bubble changes from purple, blue, green  
302 to red, and the smaller the enrichment p-value, the greater the significance.

303



304  
305  
306  
307  
308

Figure 3. Gene ontology classification in embryo toxicity test. Blue represents GO entries enriched with all genes, red represents GO entries enriched with differential genes. The horizontal axis represents the entry name, and the vertical axis represents the number (on right) and percentage of genes (on left) corresponding to the entry.

### 3.2 BMDL<sub>5</sub> estimation based on in-vitro data

309  
310 The dose-response relationship between exposure concentrations and responses of gene  
311 expressions was examined using BBMD analysis. Genes that showed a significant difference in the  
312 PCR test were included in BBMD analysis (Table 1). The Benchmark does lower confidence limit  
313 (BMDL<sub>5</sub>) values for G protein-coupled estrogen receptor 1 (GPER1) and cytochrome P450 family  
314 11 subfamily A member 1 (CYP11A1) were above 100 nM. The BMDL<sub>5</sub> value of hydroxy-delta-  
315 5-steroid dehydrogenase, 3 beta- and steroid delta-isomerase 1 (HSD3B1) was the lowest (7.24 nM).  
316 For the neurodevelopmental toxicity test, the selection of genes in the PCR array was based on  
317 previous bioinformatics analysis conducted by our group<sup>49</sup> (ESR1, ESR2, MAPK1, MAPK3,  
318 GRIN2B, GRIN1, GRIA1, ARAF, and RPS6KA2), related literature<sup>50, 51</sup> (EGR3, FABP5, PTN,  
319 POMC, NTRK2, NFATC2, NFAT5), and AOP 12  
320 ([https://aopwiki.org/aops/12#graphical\\_representation](https://aopwiki.org/aops/12#graphical_representation)) (GRIN2A, GRIN3A, GRIN2D, RCAN1,  
321 BDNF and BCL2 were chosen according to the MIE and cellular effects of AOP 12). Then genes  
322 mentioned above were selected for the analysis of variance and differential genes were further  
323 analysed using BBMD analysis. The BMDL<sub>5</sub> values of ARAF, BDNF, GRIN2A, GRIN3A and  
324 POMC are above 25000 nM. While the BMDL<sub>5</sub> values of EGR3, GRIA1, NFATC2 and NFAT5  
325 are below 500 nM.

326

**Table 1. HEDs in embryo and neurodevelopmental toxicity test**

Embryo toxicity test				
Gene	BMDL <sub>5th</sub> /nM	POD/ $\mu$ M	Cplasma-fetus/ $\mu$ M	HED (mg/kg/day)
GPER1	102.830	0.103	1.473	0.070
CGA	8.200	0.008	0.128	0.064
CYP19A1	12.870	0.013	0.200	0.064
CYP11A1	119.870	0.120	1.695	0.071
CDKN1C	63.220	0.063	0.939	0.067
CACNA1C	29.650	0.030	0.454	0.065

HSD3B1	7.240	0.007	0.113	0.064
<b>Neurodevelopmental toxicity test</b>				
Gene	BMDL <sub>5th</sub> /nM	POD/ $\mu$ M	C <sub>brain-fetus</sub> / $\mu$ M	HED (mg/kg/day)
ARAF	55153.430	55.153	232.703	0.237
BCL2	2021.400	2.021	27.411	0.074
BDNF	39962.170	39.962	188.396	0.212
EGR3	436.480	0.436	7.348	0.059
FABP5	3560.690	3.561	42.571	0.084
GRIA1	364.640	0.365	6.275	0.058
GRIN2A	25477.300	25.477	143.313	0.178
GRIN2D	1534.430	1.534	21.832	0.070
GRIN3A	36673.380	36.673	178.491	0.205
RPS6KA2	8623.050	8.623	76.863	0.112
RCAN1	6809.130	6.809	66.418	0.103
PTN	2164.240	2.164	28.969	0.075
POMC	48627.900	48.628	213.895	0.227
NTRK2	589.290	0.589	9.562	0.062
NFATC2	155.590	0.156	2.967	0.052
NFAT5	381.830	0.382	6.534	0.058

327

### 328 3.3 Extrapolation of HEDs based on P-PBPK model

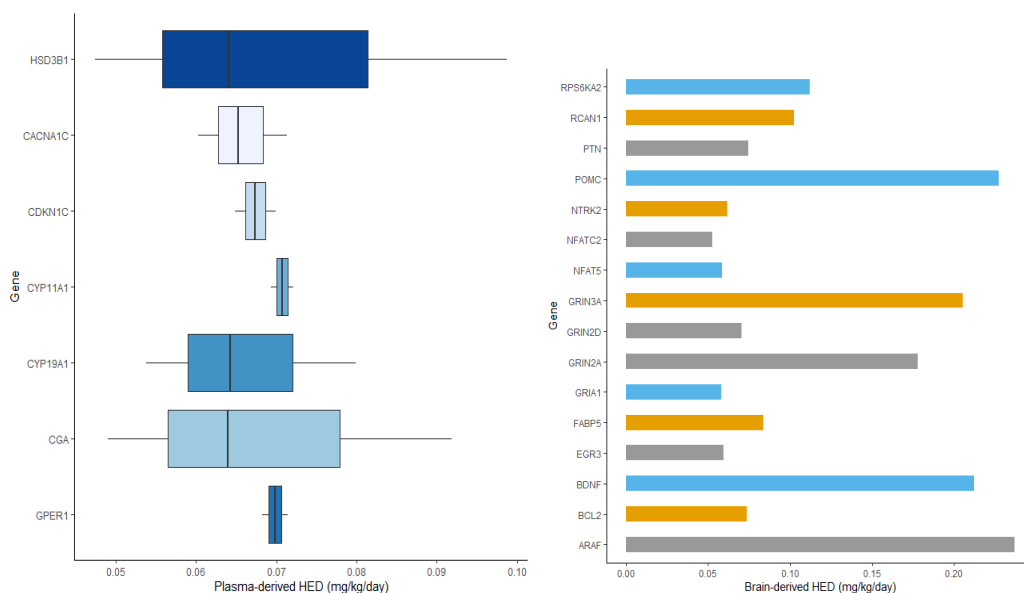
329 The reverse dosimetry using a P-PBPK model was used to calculate P2.5, P5, P50 and P97.5  
330 of the  $C_{max,ss}$  after the exposure, and HEDs using equation 1, as shown in Figure 4A, B. For plasma,  
331 the  $C_{max,ss}$  values (mean) ranged from 0.11 (HSD3B1) to 1.70 (CYP11A1)  $\mu$ M. The  $C_{max,ss}$  values  
332 (mean) calculated from the brain were higher than those of plasma. The minimum  $C_{max,ss}$  for the  
333 fetus's brain was 2.97  $\mu$ M (NFATC2) and the maximum was 232.70  $\mu$ M (ARAF). The plasma  
334  $C_{max,ss}$ -derived HEDs (mean) were comparable, ranging from 0.064 (CGA, glycoprotein hormones,  
335 alpha polypeptide) to 0.071 (CYP11A1) mg/kg/day. The brain  $C_{max,ss}$ -derived HEDs had wider  
336 ranges (0.052-0.24) (mg/kg/day) compared to the plasma  $C_{max,ss}$ -derived HEDs (0.065-0.071)  
337 (mg/kg/day).

338

339

A

B



340  
 341 Figure 4. HEDs estimation using Markov Chain Monte Carlo simulations. A: the P2.5, P50 and  
 342 P97.5 of the plasma  $C_{max,ss}$ -derived HEDs. B: the P50 of the fetus brain  $C_{max,ss}$ -derived HEDs.  
 343

### 344 3.4 Convergence achieved during reverse dosimetry

345 The convergence for MCMC simulation done to reconstruct the exposure was checked to  
 346 increase the credibility of results. The well-mixed Markov chains probabilistic density plots  
 347 (Supplementary file 2, Figure S4 and S5) for the mean ( $\mu_a$ ) and standard deviation ( $\sigma_a$ ) of  
 348 informative parameter “a” showed convergence in all simulations. A scale reduction factor ( $\hat{R}$ )  $\leq 1.00$   
 349 was achieved for all simulations and ESS tails were above 100 per chain, indicating convergence.  
 350

### 351 3.5 Risk characterization

352 The RfDs were calculated (eq.2) as the TD (The fifth percentile of HEDs) divided by 10  
 353 (uncertainty factor)<sup>35</sup>. This uncertainty factor was considered to address the pharmacokinetic  
 354 variability in ADME (absorption, distribution, metabolism and excretion) profile when moving from  
 355 in-vitro cell lines to human risk assessment. The RfDs derived from the plasma concentration ranged  
 356 from 4.94 to 6.96  $\mu\text{g}/\text{kg}\cdot\text{bw}$  per day, which are narrower than the mean RfDs estimated with brain  
 357 dosimetry (5.18-23.70  $\mu\text{g}/\text{kg}\cdot\text{bw}$  per day) (Supplementary file 2, Table S4). The RfDs are much  
 358 lower than an EFSA (2006) t-TDI of 50  $\mu\text{g}/\text{kg}\cdot\text{bw}$  per day for BPA but close to the EFSA t-TDI  
 359 updated in 2015 (4  $\mu\text{g}/\text{kg}\cdot\text{bw}$  per day). The EFSA Panel applied a total uncertainty factor of 150 to  
 360 establish a t-TDI of 4  $\mu\text{g}/\text{kg}\cdot\text{bw}$  based on the mean relative kidney weight effect in mice. As EFSA  
 361 has drastically reduced the TDI to 0.2  $\text{ng}/\text{kg}\cdot\text{bw}$  per day in the 2023 scientific opinion report<sup>25</sup>, the  
 362 t-TDI of 2015 is approximately 50 times higher compared to 2023 (TDI).

## 363 4. Discussion

364 In the present study, Bayesian dose-response analysis of human in-vitro toxicogenomic data  
 365 was combined with PBPK modeling to assess the risk of BPA in humans. Human ESCs were used  
 366 to perform in-vitro experiments to reduce the uncertainty associated with extrapolation between  
 367 different species. The H9 cell line is differentiated naturally into various types of cells and also  
 368 differentiated specifically into neurons to conduct the developmental and neurodevelopmental  
 369 toxicity test. Given the time required for differentiation and to be comparable between the two  
 370 developmental tests, the same frequency of exposure was set by us for the in-vitro experiment. The

371 dose setting in this study was based on the oral exposure of the Chinese population and a long-term  
372 (14-day) exposure of human ESCs was done to mimic long-term human exposure.

373 Transcriptomic analysis was done for embryotoxicity, and genes were selected based on  
374 AOP12, previous experiments conducted by our group<sup>49</sup> and some literature<sup>50, 51</sup>. Transcriptomics  
375 analysis for BPA showed that the DEGs were enriched in the following pathways: ovarian  
376 steroidogenesis, protein digestion and absorption, ECM-receptor interaction, PI3K-Akt signaling  
377 pathway, MAPK signaling pathway and Ras signaling pathway. Many of these pathways,  
378 particularly the last three, are involved in one or another step of the cell cycle like transcription,  
379 translation, proliferation, survival, growth, differentiation etc. pointing towards important processes  
380 of embryo development<sup>52</sup>. The ovarian steroidogenesis pathway plays a significant role in uterine  
381 function, and the establishment and maintenance of pregnancy<sup>53</sup>. These pathways may help  
382 elucidate the mechanism and explore the mode of action of BPA's embryotoxicity. However, further  
383 studies can be done to explore in detail. Further PCR test of the selected DEGs in the transcriptomics  
384 analysis revealed that the genes which showed statistical significance were mostly related to  
385 different kinds of hormones (steroid hormones: HSD3B1, glycoprotein hormones: CGA). The gene  
386 (CDKN1C) involving cell cycle also showed statistically significant among different dose groups.  
387 Combining the results of the top 20 KEGG pathways from transcriptomics analysis and cell cycle  
388 assay, ovarian steroidogenesis pathway and cell growth were found to be two major events  
389 happening after BPA exposure. Both these events may be contributing towards embryotoxicity due  
390 to BPA exposure as evidenced by altered cell cycle and decrease viability (Fig S1, S2). In the  
391 neurodevelopmental toxicity test, genes involving NMDAR (GRIN2A, GRIN3A, GRIN2D),  
392 calcineurin A (RCAN1), cell injury/death (BCL2) and encoding a member of the nerve growth factor  
393 family of proteins (BDNF) were statistically significant. The proteins associated with these genes  
394 also appear to be a part of the neurodegenerative process in an endorsed AOP (AOP12, Chronic  
395 binding of antagonist to N-methyl-D-aspartate receptors (NMDARs) during brain development  
396 leads to neurodegeneration with impairment in learning and memory in aging,  
397 <https://aopwiki.org/aops/12>). This suggests that BPA may play an important role in inducing  
398 developmental neurotoxicity, but further studies are needed to reach a conclusion. Multiple  
399 epidemiological studies have also provided evidence with early BPA exposure and  
400 neurodevelopmental disorders like attention deficit/hyperactive disorder and autism spectrum  
401 disorder<sup>54</sup>. We also used in-vitro data along with in-silico models to estimate POD, HED and RfD  
402 for human risk assessment.

403 Bayesian BMD is considered as a preferred method for dose-response evaluation<sup>55</sup> to  
404 investigate the relationship between intracellular concentrations and the toxicogenomic response to  
405 obtain POD. The genes with the lowest BMDL for embryotoxicity and neurodevelopmental toxicity  
406 test were HSD3B1 and NFATC2, respectively. The protein encoded by HSD3B1 is an enzyme that  
407 can catalyze and produce all classes of steroid hormones<sup>56</sup>. The nuclear factor of activated T cells 2  
408 (NFATC2) is a member of the nuclear factor of the activated T cells (NFAT) family and plays a  
409 central role in inducing gene transcription during the immune response<sup>57</sup>.

410 The calculated BMD<sub>5</sub> was used as input for the P-PBPK-IVIVE approach to predict the HED  
411 which was then extrapolated to calculate the RfD. Lin et al<sup>37</sup> conducted a population-based IVIVE  
412 using PBPK models coupled with Monte Carlo simulations to convert ToxCast in vitro ER assays  
413 of BPA, BPS, BPF and BPAF to HEDs. The HED for the ER gene transcription was 0.40 mg/kg/day  
414 for BPA, which is much more higher than the HEDs calculated in the present study. The reason  
415 behind this is the different endpoints considered to derive HEDs. Even though the disruption of the  
416 ER is a major concern for risk assessment<sup>58</sup> the toxicity mechanism of BPA has not been fully

417 elucidated. Further research is necessary to explore more biological processes and sensitive  
418 endpoints to fully understand the toxicity mechanism of BPA and obtain more accurate HEDs. The  
419 RfD was calculated based on the DEGs which may be involved directly or indirectly in the BPA-  
420 induced toxicity. The result shows that the DEGs for the embryo and neurodevelopment are different,  
421 but the minimum RfDs derived from the plasma and brain dosimetry are similar. However, the  
422 maximum RfD derived from the brain dosimetry is three times that derived from plasma dosimetry,  
423 which explains the variation in sensitivities of different genes. For RfD analysis, NFATC2 also  
424 shows the lowest value among all the selected genes like BMDL.

425 The RfD of the most sensitive gene related to neurotoxicity (NFATC2, 5.2  $\mu\text{g}/\text{kg}/\text{day}$ ) was close to  
426 the EFSA's 2015 t-TDI. However, the current derived RfDs are below the estimated dietary  
427 exposures of BPA in European and Chinese populations. Dietary exposures to BPA in European  
428 populations were estimated on average to 81  $\mu\text{g}/\text{kg}\cdot\text{bw}/\text{d}$  for children, 55  $\mu\text{g}/\text{kg}\cdot\text{bw}/\text{d}$  for adolescents  
429 and 42  $\mu\text{g}/\text{kg}\cdot\text{bw}/\text{d}$  for adults between 45 and 65 years old<sup>22</sup>. According to the fifth Chinese TDS,  
430 the mean dietary exposure to BPA was 200.955  $\text{ng}/\text{kg}\cdot\text{bw}/\text{d}$  for adults above 19 years old<sup>40</sup>. In recent  
431 EFSA's scientific opinion of BPA<sup>25</sup>, EFSA established a TDI of 0.2  $\text{ng}/\text{kg}\cdot\text{bw}$  based on the effect  
432 on Th17 cells in mice. This means that simulated RfD is more than 1000 times higher than TDI.  
433 However, there may be some uncertainty in calculating the RfD. For instance, consideration of  
434 uncertainty factor of 10 to account for undefined variability like genetic polymorphism, individual  
435 differences etc. Currently, there is no established method for interspecies extrapolating  
436 toxicogenomic data as there are no unified standards to use toxicogenomic data to estimate RfDs.  
437 Another limitation can be that during dosimetry IVIVE, we considered Cmax but instead AUC can  
438 be taken as standard. This is an ongoing discussion among experts and needs further reviewing  
439 before coming to concrete decisions. While doing in-vitro studies, we assumed that the applied  
440 exposure is the actual concentration in the cell, but this may not hold true. Some compounds may  
441 bind to plastic or degrade, reducing the overall active concentration. This requires further  
442 investigations and some in-vitro PBPK model can be developed to reduce the uncertainty. However,  
443 this study is a starting point to extrapolate in-vitro toxicogenomic data by in-silico rather than animal  
444 experiments, which is a step towards NAM. This NAM is not limited to the type of contaminants as  
445 long as there is a PBPK model and in-vitro data for the target contaminant.

446 However, there are some limitations of this study. We considered dietary exposure for adult  
447 female and not for pregnant females which can be one of the uncertainties in the prediction. The  
448 BMD analysis took the PCR data to conduct the dose-response evaluation. However, a gene is  
449 usually involved in several pathways, which makes it ambiguous to determine the most significant  
450 one. And gene expression changes may not lead to a clear adverse toxicological effect. Thus, the  
451 association between gene expression changes and adverse outcomes is not well understood and  
452 explained and using toxicogenomic data for risk assessment is still difficult. Nevertheless, the genes  
453 selected in our study were based on the PCR test, transcriptomics analysis and previous  
454 bioinformatic analysis, which reduced the uncertain causality. Another major limitation is that the  
455 in-vitro study done for short-time interval may not represent human long-term exposure. This is an  
456 open question to be resolved by the scientific community. The exposure pathway simulated in this  
457 study is oral exposure. However, dermal and inhalation exposure can also be considered when  
458 exposure data will become available. The P-PBPK model for fetus did not consider gender  
459 differences due to limited data availability for such a population. However, the model can be further  
460 extended if required. The prediction results of risk assessment for pregnant women can be different  
461 for other age groups as pregnant women and fetuses have different physiology. However, the  
462 reference dose calculated for pregnant females can be extended for other age-groups using the life-

463 stage PBPK model.

## 464 5. Conclusion

465 We conducted human-embryonic-cell-based in-vitro experiments and then integrated  
466 toxicogenomic dose-response data and IVIVE-PBPK for the human health risk assessment of BPA.  
467 The in-vitro study suggests that steroid hormones might be one of the factor contributing to BPA's  
468 embryotoxicity while the immune response-related gene was found to be the most sensitive in the  
469 neurodevelopmental toxicity test. The RfDs were derived from DEGs showing significant  
470 differences in the embryotoxicity/neurotoxicity test. The simulated RfD for the most sensitive gene  
471 was closer to the EU guidance value (t-TDI: 4 µg/kg·bw) recommended by EFSA in 2015. However,  
472 these are results from specific in-vitro cell lines and there are some uncertainties which may be  
473 present while considering simulated RfD for any regulatory purpose. The simulated RfD is  
474 considerably high compared to the EFSA TDI established in 2023 for a different endpoint  
475 (immunotoxicity). This study has also shown the application of an IVIVE-PBPK-based NAM which  
476 can be applied to other chemicals to conduct risk assessments and improve public health decisions.

## 477 Acknowledgement

478 The first author is partially supported by the grant CSC #202106240169 from the P. R. China.  
479 Translational modelling, data analysis and manuscript writing have partially been supported by the  
480 funding from the European Union's Horizon 2020 research and innovation program under grant  
481 agreement No. 101057014 (PARC).

## 482 Conflict of interests

483 The authors declare no competing financial interest.

## 484 Data Availability

485 The code used in the work is available at [InSilicoVida/Toxicogenomic-in-BPA-with-PBPK: IVIVE-](https://github.com/InSilicoVida/Toxicogenomic-in-BPA-with-PBPK)  
486 [P-PBPK for extrapolating risk from in-vitro to human health especially for DNT \(github.com\)](https://github.com/InSilicoVida/Toxicogenomic-in-BPA-with-PBPK). The  
487 data generated from in-vitro study like transcriptomic data is provided as per OECD reporting  
488 framework. The raw sequencing data, mapped data, and data for visualization of the RNA-Seq  
489 analyses of the embryonic stem cell with exposure to 10 µM BPA for 14 days transcriptome data  
490 have been deposited in the Bioproject at the National Center for Biotechnology Information (NCBI)  
491 under accession number PRJNA998583.

## 492 Abbreviations

Abbreviations	Definition
AUC	Area under the curve
BBMD	Bayesian benchmark dose
BMD	Benchmark dose
BMDL	Benchmark does lower confidence limit
BMR	Benchmark response
BPA	Bisphenol A
C <sub>max,ss</sub>	Maximum steady-state concentration
CYP11A1	Cytochrome P450 family 11 subfamily A member 1

---

DEGs	Differentially expressed genes
DMSO	Dimethyl sulfoxide
DNT	Developmental neurotoxicity
EBs	Embryonic Bodies
EDC	Endocrine-disrupting chemical
EFSA	European Food Safety Authority
ER	Estrogen receptor
ESCs	Embryonic stem cells
FDA	Food and Drug Administration
GD	Gestation day
GO	Gene Ontology
GPER1	G protein-coupled estrogen receptor 1
HEDs	Human equivalent doses
HSD3B1	Hydroxy-delta-5-steroid dehydrogenase, 3 beta- and steroid delta-isomerase 1
IVIVE	In vitro-in vivo extrapolation
KEGG	Kyoto Encyclopedia of Genes and Genomes
MCMC	Markov chain Monte Carlo
NAM	New approach methodology
NFAT	Nuclear factor of the activated T cells
NMDARs	N-methyl-D-aspartate receptors
PI3K	Phosphatidylinositol 3-kinase
POD	Point of departure
P-PBPK	Pregnancy physiologically based pharmacokinetic model
RfD	Reference dose
SML	Specific migration limit
TD	Threshold dose
TDI	Tolerable daily intake
t-TDI	Temporary-tolerable daily intake
TDS	Total diet study

---

## 493 References

- 506 1. Matuszczak, E.; Komarowska, M. D.; Debek, W.; Hermanowicz, A., The Impact of Bisphenol  
507 A on Fertility, Reproductive System, and Development: A Review of the Literature. *International*  
508 *journal of endocrinology* **2019**, *2019*, 4068717.
- 509 2. Gimeno, P.; Spinau, C.; Lassu, N.; Maggio, A. F.; Brenier, C.; Lempereur, L., Identification and  
510 quantification of bisphenol A and bisphenol B in polyvinylchloride and polycarbonate medical  
511 devices by gas chromatography with mass spectrometry. *Journal of separation science* **2015**, *38*  
512 (21), 3727-34.
- 513 3. Dursun, E.; Fron-Chabouis, H.; Attal, J. P.; Raskin, A., Bisphenol A Release: Survey of the  
514 Composition of Dental Composite Resins. *The open dentistry journal* **2016**, *10*, 446-453.
- 515 4. Hahladakis, J. N.; Iacovidou, E.; Gerassimidou, S., An overview of the occurrence, fate, and

- 516 human risks of the bisphenol-A present in plastic materials, components, and products. *Integrated*  
517 *environmental assessment and management* **2023**, *19* (1), 45-62.
- 518 5. Torres-García, J. L.; Ahuactzin-Pérez, M.; Fernández, F. J.; Cortés-Espinosa, D. V., Bisphenol  
519 A in the environment and recent advances in biodegradation by fungi. *Chemosphere* **2022**, *303*  
520 (Pt 1), 134940.
- 521 6. Lesser, L. E.; Mora, A.; Moreau, C.; Mahlke, J.; Hernández-Antonio, A.; Ramírez, A. I.;  
522 Barrios-Piña, H., Survey of 218 organic contaminants in groundwater derived from the world's  
523 largest untreated wastewater irrigation system: Mezquital Valley, Mexico. *Chemosphere* **2018**, *198*,  
524 510-521.
- 525 7. Dan, L.; Wu, S.; Xu, H.; Zhang, Q.; Zhang, S.; Shi, L.; Yao, C.; Liu, Y.; Cheng, J., Distribution  
526 and bioaccumulation of endocrine disrupting chemicals in water, sediment and fishes in a shallow  
527 Chinese freshwater lake: Implications for ecological and human health risks. *Ecotoxicology and*  
528 *environmental safety* **2017**, *140*, 222-229.
- 529 8. Sun, Q.; Wang, Y.; Li, Y.; Ashfaq, M.; Dai, L.; Xie, X.; Yu, C. P., Fate and mass balance of  
530 bisphenol analogues in wastewater treatment plants in Xiamen City, China. *Environmental*  
531 *pollution (Barking, Essex : 1987)* **2017**, *225*, 542-549.
- 532 9. Geens, T.; Aerts, D.; Berthot, C.; Bourguignon, J. P.; Goeyens, L.; Lecomte, P.; Maghuin-  
533 Rogister, G.; Pironnet, A. M.; Pussemier, L.; Scippo, M. L.; Van Loco, J.; Covaci, A., A review of  
534 dietary and non-dietary exposure to bisphenol-A. *Food and chemical toxicology : an international*  
535 *journal published for the British Industrial Biological Research Association* **2012**, *50* (10), 3725-40.
- 536 10. Ribeiro, E.; Ladeira, C.; Viegas, S., Occupational Exposure to Bisphenol A (BPA): A Reality That  
537 Still Needs to Be Unveiled. *Toxics* **2017**, *5* (3).
- 538 11. Sabuz Vidal, O.; Deepika, D.; Schuhmacher, M.; Kumar, V., EDC-induced mechanisms of  
539 immunotoxicity: a systematic review. *Critical reviews in toxicology* **2021**, *51* (7), 634-652.
- 540 12. Ni, M.; Li, X.; Zhang, L.; Kumar, V.; Chen, J., Bibliometric Analysis of the Toxicity of Bisphenol  
541 A. *International journal of environmental research and public health* **2022**, *19* (13).
- 542 13. Ma, Y.; Liu, H.; Wu, J.; Yuan, L.; Wang, Y.; Du, X.; Wang, R.; Marwa, P. W.; Petlulu, P.; Chen,  
543 X.; Zhang, H., The adverse health effects of bisphenol A and related toxicity mechanisms.  
544 *Environmental research* **2019**, *176*, 108575.
- 545 14. Vandenberg, L. N.; Chahoud, I.; Heindel, J. J.; Padmanabhan, V.; Paumgarten, F. J.;  
546 Schoenfelder, G., Urinary, circulating, and tissue biomonitoring studies indicate widespread  
547 exposure to bisphenol A. *Environmental health perspectives* **2010**, *118* (8), 1055-70.
- 548 15. Barraza, L., A new approach for regulating bisphenol A for the protection of the public's health.  
549 *The Journal of law, medicine & ethics : a journal of the American Society of Law, Medicine & Ethics*  
550 **2013**, *41 Suppl 1*, 9-12.
- 551 16. Wiraagni, I. A.; Mohd, M. A.; Bin Abd Rashid, R.; Haron, D., Validation of a simple extraction  
552 procedure for bisphenol A identification from human plasma. *PloS one* **2019**, *14* (10), e0221774.
- 553 17. Liu, J.; Yu, P.; Qian, W.; Li, Y.; Zhao, J.; Huan, F.; Wang, J.; Xiao, H., Perinatal bisphenol A  
554 exposure and adult glucose homeostasis: identifying critical windows of exposure. *PloS one* **2013**,  
555 *8* (5), e64143.
- 556 18. Namat, A.; Xia, W.; Xiong, C.; Xu, S.; Wu, C.; Wang, A.; Li, Y.; Wu, Y.; Li, J., Association of  
557 BPA exposure during pregnancy with risk of preterm birth and changes in gestational age: A meta-  
558 analysis and systematic review. *Ecotoxicology and environmental safety* **2021**, *220*, 112400.
- 559 19. Chen, D.; Kannan, K.; Tan, H.; Zheng, Z.; Feng, Y. L.; Wu, Y.; Widelka, M., Bisphenol

560 Analogues Other Than BPA: Environmental Occurrence, Human Exposure, and Toxicity-A Review.  
561 *Environmental science & technology* **2016**, *50* (11), 5438-53.

562 20. Liao, C.; Kannan, K., Concentrations and profiles of bisphenol A and other bisphenol  
563 analogues in foodstuffs from the United States and their implications for human exposure. *Journal*  
564 *of agricultural and food chemistry* **2013**, *61* (19), 4655-62.

565 21. Baluka, S. A.; Rumbelha, W. K., Bisphenol A and food safety: Lessons from developed to  
566 developing countries. *Food and chemical toxicology : an international journal published for the*  
567 *British Industrial Biological Research Association* **2016**, *92*, 58-63.

568 22. Journal, E. F. S. A. J. E., Opinion of the Scientific Panel on food additives, flavourings,  
569 processing aids and materials in contact with food (AFC) related to 2, 2-bis (4-hydroxyphenyl)  
570 propane bis (2, 3-epoxypropyl) ether (Bisphenol A diglycidyl ether, BADGE). REF. No 13510 and  
571 39700. **2004**, *2* (7), 86.

572 23. Authority, E. J. E. J., Scientific opinion on the risks to public health related to the presence of  
573 bisphenol A (BPA) in foodstuffs. **2015**, *13* (1).

574 24. Luo, S.; Li, Y.; Li, Y.; Zhu, Q.; Jiang, J.; Wu, C.; Shen, T., Gestational and lactational exposure  
575 to low-dose bisphenol A increases Th17 cells in mice offspring. *Environmental toxicology and*  
576 *pharmacology* **2016**, *47*, 149-158.

577 25. Lambré, C.; Barat Baviera, J. M.; Bolognesi, C.; Chesson, A.; Cocconcelli, P. S.; Crebelli, R.;  
578 Gott, D. M.; Grob, K.; Lampi, E.; Mengelers, M.; Mortensen, A.; Rivière, G.; Silano Until December,  
579 V.; Steffensen, I. L.; Tlustos, C.; Vernis, L.; Zorn, H.; Batke, M.; Bignami, M.; Corsini, E.; FitzGerald,  
580 R.; Gundert-Remy, U.; Halldorsson, T.; Hart, A.; Ntzani, E.; Scanziani, E.; Schroeder, H.; Ulbrich,  
581 B.; Waalkens-Berendsen, D.; Woelfle, D.; Al Harraq, Z.; Baert, K.; Carfi, M.; Castoldi, A. F.; Croera,  
582 C.; Van Loveren, H., Re-evaluation of the risks to public health related to the presence of bisphenol  
583 A (BPA) in foodstuffs. *EFSA journal. European Food Safety Authority* **2023**, *21* (4), e06857.

584 26. Laroche, C.; Aggarwal, M.; Bender, H.; Benndorf, P.; Birk, B.; Crozier, J.; Dal Negro, G.; De  
585 Gaetano, F.; Desaintes, C.; Gardner, I.; Hubesch, B.; Irizar, A.; John, D.; Kumar, V.; Lostia, A.;  
586 Manou, I.; Monshouwer, M.; Müller, B. P.; Paini, A.; Reid, K.; Rowan, T.; Sachana, M.; Schutte,  
587 K.; Stirling, C.; Taalman, R.; van Aerts, L.; Weissenhorn, R.; Sauer, U. G., Finding synergies for 3Rs  
588 - Toxicokinetics and read-across: Report from an EPAA partners' Forum. *Regulatory toxicology*  
589 *and pharmacology : RTP* **2018**, *99*, 5-21.

590 27. Deepika, D.; Sharma, R. P.; Schuhmacher, M.; Kumar, V. J. C. R. i. T., An integrative  
591 translational framework for chemical induced neurotoxicity—a systematic review. **2020**, *50* (5), 424-  
592 438.

593 28. Martin, G. R., Isolation of a pluripotent cell line from early mouse embryos cultured in medium  
594 conditioned by teratocarcinoma stem cells. *Proceedings of the National Academy of Sciences of*  
595 *the United States of America* **1981**, *78* (12), 7634-8.

596 29. Seiler, A. E.; Spielmann, H., The validated embryonic stem cell test to predict embryotoxicity  
597 in vitro. *Nature protocols* **2011**, *6* (7), 961-78.

598 30. Krewski, D.; Acosta, D., Jr.; Andersen, M.; Anderson, H.; Bailar, J. C., 3rd; Boekelheide, K.;  
599 Brent, R.; Charnley, G.; Cheung, V. G.; Green, S., Jr.; Kelsey, K. T.; Kerkvliet, N. I.; Li, A. A.; McCray,  
600 L.; Meyer, O.; Patterson, R. D.; Pennie, W.; Scala, R. A.; Solomon, G. M.; Stephens, M.; Yager, J.;  
601 Zeise, L., Toxicity testing in the 21st century: a vision and a strategy. *Journal of toxicology and*  
602 *environmental health. Part B, Critical reviews* **2010**, *13* (2-4), 51-138.

603 31. Council, N. R., *Toxicity testing in the 21st century: a vision and a strategy*. National Academies

604 Press: 2007.

605 32. Rotroff, D. M.; Wetmore, B. A.; Dix, D. J.; Ferguson, S. S.; Clewell, H. J.; Houck, K. A.; Lecluyse,  
606 E. L.; Andersen, M. E.; Judson, R. S.; Smith, C. M.; Sochaski, M. A.; Kavlock, R. J.; Boellmann, F.;  
607 Martin, M. T.; Reif, D. M.; Wambaugh, J. F.; Thomas, R. S., Incorporating human dosimetry and  
608 exposure into high-throughput in vitro toxicity screening. *Toxicological sciences : an official journal*  
609 *of the Society of Toxicology* **2010**, *117*(2), 348-58.

610 33. Wetmore, B. A., Quantitative in vitro-to-in vivo extrapolation in a high-throughput  
611 environment. *Toxicology* **2015**, *332*, 94-101.

612 34. Wetmore, B. A.; Wambaugh, J. F.; Ferguson, S. S.; Sochaski, M. A.; Rotroff, D. M.; Freeman,  
613 K.; Clewell, H. J., 3rd; Dix, D. J.; Andersen, M. E.; Houck, K. A.; Allen, B.; Judson, R. S.; Singh, R.;  
614 Kavlock, R. J.; Richard, A. M.; Thomas, R. S., Integration of dosimetry, exposure, and high-  
615 throughput screening data in chemical toxicity assessment. *Toxicological sciences : an official*  
616 *journal of the Society of Toxicology* **2012**, *125*(1), 157-74.

617 35. Chen, Q.; Chou, W. C.; Lin, Z., Integration of Toxicogenomics and Physiologically Based  
618 Pharmacokinetic Modeling in Human Health Risk Assessment of Perfluorooctane Sulfonate.  
619 *Environmental science & technology* **2022**, *56*(6), 3623-3633.

620 36. Zhang, Y.; Liu, Z.; Wang, Z.; Gao, H.; Wang, Y.; Cui, M.; Peng, H.; Xiao, Y.; Jin, Y.; Yu, D.;  
621 Chen, W.; Wang, Q., Health risk assessment of cadmium exposure by integration of an in silico  
622 physiologically based toxicokinetic model and in vitro tests. *Journal of hazardous materials* **2023**,  
623 *443*(Pt A), 130191.

624 37. Lin, Y. J.; Lin, Z., In vitro-in silico-based probabilistic risk assessment of combined exposure  
625 to bisphenol A and its analogues by integrating ToxCast high-throughput in vitro assays with in  
626 vitro to in vivo extrapolation (IVIVE) via physiologically based pharmacokinetic (PBPK) modeling.  
627 *Journal of hazardous materials* **2020**, *399*, 122856.

628 38. Sharma, R. P.; Schuhmacher, M.; Kumar, V., The development of a pregnancy PBPK Model  
629 for Bisphenol A and its evaluation with the available biomonitoring data. *The Science of the total*  
630 *environment* **2018**, *624*, 55-68.

631 39. Martínez, M.; González, N.; Martí, A.; Marquès, M.; Rovira, J.; Kumar, V.; Nadal, M., Human  
632 biomonitoring of bisphenol A along pregnancy: An exposure reconstruction of the EXHES-Spain  
633 cohort. *Environmental research* **2021**, *196*, 110941.

634 40. Yao, K.; Zhang, J.; Yin, J.; Zhao, Y.; Shen, J.; Jiang, H.; Shao, B., Bisphenol A and Its Analogues  
635 in Chinese Total Diets: Contaminated Levels and Risk Assessment. *Oxidative medicine and cellular*  
636 *longevity* **2020**, *2020*, 8822321.

637 41. Commission, C. N. H., Report on nutrition and chronic-diseases of Chinese residents. **2020**.

638 42. Fang, H.; Zhi, Y.; Yu, Z.; Lynch, R. A.; Jia, X. J. F. C., The embryonic toxicity evaluation of  
639 deoxynivalenol (DON) by murine embryonic stem cell test and human embryonic stem cell test  
640 models. **2018**, *86*, 234-240.

641 43. Kanehisa, M.; Araki, M.; Goto, S.; Hattori, M.; Hirakawa, M.; Itoh, M.; Katayama, T.;  
642 Kawashima, S.; Okuda, S.; Tokimatsu, T.; Yamanishi, Y., KEGG for linking genomes to life and the  
643 environment. *Nucleic acids research* **2008**, *36*(Database issue), D480-4.

644 44. Shao, K.; Shapiro, A. J., A Web-Based System for Bayesian Benchmark Dose Estimation.  
645 *Environmental health perspectives* **2018**, *126*(1), 017002.

646 45. Committee, E. S.; Hardy, A.; Benford, D.; Halldorsson, T.; Jeger, M. J.; Knutsen, K. H.; More,  
647 S.; Mortensen, A.; Naegeli, H.; Noteborn, H. J. E. J., Update: use of the benchmark dose approach

648 in risk assessment. **2017**, *15*(1), e04658.

649 46. Chou, W. C.; Lin, Z., Probabilistic human health risk assessment of perfluorooctane sulfonate  
650 (PFOS) by integrating in vitro, in vivo toxicity, and human epidemiological studies using a  
651 Bayesian-based dose-response assessment coupled with physiologically based pharmacokinetic  
652 (PBPK) modeling approach. *Environment international* **2020**, *137*, 105581.

653 47. Bell, S. M.; Chang, X.; Wambaugh, J. F.; Allen, D. G.; Bartels, M.; Brouwer, K. L. R.; Casey,  
654 W. M.; Choksi, N.; Ferguson, S. S.; Fraczkiwicz, G.; Jarabek, A. M.; Ke, A.; Lumen, A.; Lynn, S.  
655 G.; Paini, A.; Price, P. S.; Ring, C.; Simon, T. W.; Sipes, N. S.; Sprankle, C. S.; Strickland, J.;  
656 Troutman, J.; Wetmore, B. A.; Kleinstreuer, N. C., In vitro to in vivo extrapolation for high  
657 throughput prioritization and decision making. *Toxicology in vitro : an international journal*  
658 *published in association with BIBRA* **2018**, *47*, 213-227.

659 48. Gelman, S. A., Psychological essentialism in children. *Trends in cognitive sciences* **2004**, *8*(9),  
660 404-9.

661 49. Li, X.; Ni, M.; Yang, Z.; Chen, X.; Zhang, L.; Chen, J., Bioinformatics analysis and quantitative  
662 weight of evidence assessment to map the potential mode of actions of bisphenol A.  
663 *Environmental pollution (Barking, Essex : 1987)* **2021**, *273*, 116469.

664 50. Li, J.; Fu, K. Z.; Vemula, S.; Le, X. C.; Li, X. F., Studying developmental neurotoxic effects of  
665 bisphenol A (BPA) using embryonic stem cells. *Journal of environmental sciences (China)* **2015**, *36*,  
666 173-7.

667 51. Huang, B.; Jiang, C.; Luo, J.; Cui, Y.; Qin, L.; Liu, J., Maternal exposure to bisphenol A may  
668 increase the risks of Parkinson's disease through down-regulation of fetal IGF-1 expression.  
669 *Medical hypotheses* **2014**, *82*(3), 245-9.

670 52. Rossant, J.; Tam, P. P. L., Early human embryonic development: Blastocyst formation to  
671 gastrulation. *Developmental cell* **2022**, *57*(2), 152-165.

672 53. Stocco, D. M.; Wang, X.; Jo, Y.; Manna, P. R., Multiple signaling pathways regulating  
673 steroidogenesis and steroidogenic acute regulatory protein expression: more complicated than  
674 we thought. *Molecular endocrinology (Baltimore, Md.)* **2005**, *19*(11), 2647-59.

675 54. Welch, C.; Mulligan, K., Does Bisphenol A Confer Risk of Neurodevelopmental Disorders?  
676 What We Have Learned from Developmental Neurotoxicity Studies in Animal Models. *International*  
677 *journal of molecular sciences* **2022**, *23*(5).

678 55. Davis, J. A.; Gift, J. S.; Zhao, Q. J. J. T.; pharmacology, a., Introduction to benchmark dose  
679 methods and US EPA's benchmark dose software (BMDS) version 2.1. 1. **2011**, *254*(2), 181-191.

680 56. Dickson, A.; Yutuc, E.; Thornton, C. A.; Dunford, J. E.; Oppermann, U.; Wang, Y.; Griffiths,  
681 W. J., HSD3B1 is an oxysterol 3 $\beta$ -hydroxysteroid dehydrogenase in human placenta. *Open biology*  
682 **2023**, *13*(5), 220313.

683 57. Jakobi, M.; Kiefer, A.; Mirzakhani, H.; Rauh, M.; Zimmermann, T.; Xepapadaki, P.; Stanic, B.;  
684 Akdis, M.; Papadopoulos, N. G.; Raby, B. A.; Weiss, S. T.; Finotto, S., Role of nuclear factor of  
685 activated T cells 2 (NFATc2) in allergic asthma. *Immunity, inflammation and disease* **2020**, *8*(4),  
686 704-712.

687 58. Miller, M. M.; McMullen, P. D.; Andersen, M. E.; Clewell, R. A., Multiple receptors shape the  
688 estrogen response pathway and are critical considerations for the future of in vitro-based risk  
689 assessment efforts. *Critical reviews in toxicology* **2017**, *47*(7), 564-580.

690